Micro-Raman and X-ray diffraction study of Y2BaNi1−xMxO5 (M=Mg, Zn) polymorphs

ARTICLE *in* SOLID STATE COMMUNICATIONS · JUNE 2002

Impact Factor: 1.9 · DOI: 10.1016/S0038-1098(02)00168-0

4 AUTHORS, INCLUDING:

Marcella Bini
University of Pavia
76 PUBLICATIONS **1,262** CITATIONS
SEE PROFILE

V. Massarotti
University of Pavia
116 PUBLICATIONS **1,525** CITATIONS
SEE PROFILE

Pietro Galinetto
University of Pavia
128 PUBLICATIONS **873** CITATIONS
SEE PROFILE

PERGAMON

Solid State Communications 122 (2002) 367–372

solid state communications

www.elsevier.com/locate/ssc

Micro-Raman and X-ray diffraction study of $Y_2BaNi_{1-x}M_xO_5$ (M = Mg, Zn) polymorphs

D. Capsoni[a], M. Bini[a], V. Massarotti[a,*], P. Galinetto[b]

[a]*Dipartimento di Chimica Fisica, 'M. Rolla' e CSTE-CNR, viale Taramelli 16, 27100 Pavia, Italy*
[b]*INFM—Dipartimento di Fisica, 'Alessandro Volta', via Bassi 6, 27100 Pavia, Italy*

Received 12 March 2002; accepted 4 April 2002 by P. Wachter

Abstract

The Y_2BaNiO_5 compound, prototypical Haldane system characterized by anti-ferromagnetic behaviour, and its analogs $Y_2BaNi_{1-x}M_xO_5$ (M = Mg, Zn; $0.05 \leq x \leq 0.65$) are investigated by X-ray diffraction and Raman spectroscopy. Structural features and phase stability ranges of the doped samples are first determined. The first order Raman scattering for the different solid solutions is measured at room temperature in order to gain new insight on lattice dynamics of the Y_2BaNiO_5 compound when Zn^{2+} or Mg^{2+} ions progressively substitute into Ni site.

In the case of Mg substitution, the *Immm* space group (sg) showing NiO_6 octahedra (C-6) is preserved; only a very slight lattice expansion is produced and the Raman spectrum remains practically unchanged.

In Zn^{2+} doped samples, both *Immm* and *Pnma* sgs coexist in samples with $x \leq 0.13$, while for higher x values only the *Pnma* structure, having NiO_5 pyramidal coordination (C-5), is present. Such a transformation is suitably observed through the changes in the Raman spectra. In particular, the lack of the inversion symmetry on the metal ion site causes the appearance of peculiar Raman modes in the frequency region between 260 and 340 cm^{-1}. Energy and intensity of these modes are discussed taking into account the role of the doping level and of the phase abundances of the samples. The observed behaviour allows us to discuss a possible assignment of the modes in connection with the preferred insertion of Zn^{2+} in the C-5 polyhedra. © 2002 Published by Elsevier Science Ltd.

PACS: 61.10.Nz; 61.50.Ks; 78.30. − j

Keywords: E. Raman spectroscopy; C. X-ray diffraction; D. Solid phase transition

1. Introduction

Y_2BaNiO_5 is a widely studied material in recent years because of its anti-ferromagnetic behaviour (1D Heisenberg AF), with a Haldane gap from singlet ground to triplet excited state of about 10.0 meV [1,2]. The crystal structure of Y_2BaNiO_5 belongs to the orthorhombic *Immm* space group (sg) and consists of 1D chains of NiO_6 octahedra connected by the apical oxygen (O(2)) along the *a*-axis and with the basal plane formed by O(1) oxygens. The octahedra are flattened with short Ni–O(2) distances around 1.88 Å which are very unusual bond lengths for this type of oxides [3].

A lot of spectroscopic and structural studies have been devoted to investigate both Y_2BaNiO_5 [4–6] and R_2BaMO_5 (R = Y, rare earth; M = Ni, Cu, Zn) compounds [7–12]. The cited papers deal with two orthorhombic polymorphs for R_2BaMO_5 materials depending on R and M ions. The first polymorph, with MO_6 octahedra (C-6), is pertinent to Y_2BaNiO_5 compound while the other structure shows MO_5 pyramidal coordination (C-5): in this last case the structure crystallizes in the *Pnma* sg and the peculiar 1D Heisenberg anti-ferromagnetism is lost.

The bond character and related physical and chemical properties of R_2BaNiO_5 compounds may be tuned by doping with suitable cations: for example in Y_2BaNiO_5 Y^{3+} ions can be widely substituted with Ca^{2+} ions [3,13,14] and Ni^{2+} with non-magnetic divalent ions such as Mg^{2+} and Zn^{2+} [15–18].

* Corresponding author. Fax: +39-382-507575.
E-mail address: vimas@chifis.unipv.it (V. Massarotti).

0038-1098/02/$ - see front matter © 2002 Published by Elsevier Science Ltd.
PII: S0038-1098(02)00168-0

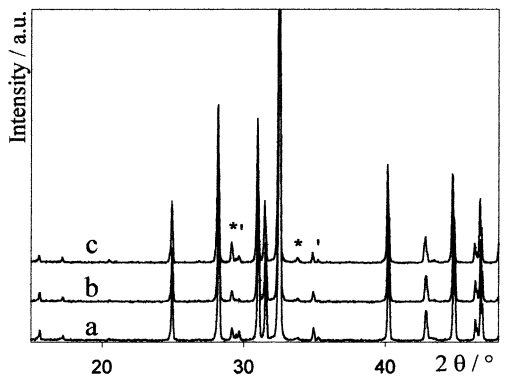

Fig. 1. XRD patterns of Mg doped samples: (a) $x = 0.05$, (b) $x = 0.10$ and (c) $x = 0.30$. The symbols indicate the main peaks of Y_2O_3 ($*$) and Y_2BaO_4 (') impurity phases.

For what concerns Zn^{2+} doped samples, both C-5 and C-6 polymorphs coexist in $Y_2BaNi_{1-x}Zn_xO_5$ samples with $x \leq 0.13$, while for higher x values only the *Pnma* structure is present [19].

Aim of the present work is to investigate the polycrystalline samples of Mg and Zn doped Y_2BaNiO_5 compound in a wide composition range ($0 \leq x \leq 0.65$) using X-ray diffraction (XRD) and micro-Raman techniques, to determine structural features, vibrational spectra and phase stability range of the doped samples. In particular, the Raman modes for the different solid solutions will be discussed in order to gain new insight on lattice dynamics of Y_2BaNiO_5 family when the Zn or Mg ions progressively substitute into Ni site.

2. Experimental

The samples have been prepared by solid-state reaction from a mixture of Y_2O_3/$BaCO_3$/NiO/MO (M = Zn, Mg) in the proper amount to obtain $Y_2BaNi_{1-x}M_xO_5$ with $0 \leq x \leq 0.65$. The mixtures have been first heated at 950 °C for 12 h to decompose the carbonate, then milled and reheated at 1100 °C for 24 h and at 1200 °C at least for 48 h (heating rate of 5 °C min^{-1}), in order to reduce the impurity amount of Y_2O_3 and Y_2BaO_4.

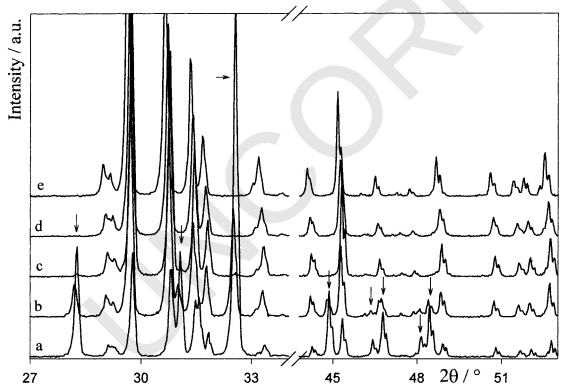

Fig. 2. Selected angular regions of XRD patterns of Zn doped samples: (a) $x = 0.05$, (b) $x = 0.10$, (c) $x = 0.15$, (d) $x = 0.30$ and (e) $x = 0.65$. The peaks of C-6 phase are indicated by arrows.

XRD patterns were performed with a Philips PW1710 diffractometer with a vertical goniometer and a curved graphite monochromator on the diffracted beam. The data were collected with the Cu Kα radiation in the 10–130° angular range. Structural and profile parameters refinement was carried out by means of the Rietveld method [20] using the FULLPROF program [21]; the parameters were varied following the procedure described elsewhere [22]. This approach allowed us to evaluate both phase abundance in multi-phase system and the occupancy of the Mg ions on the Ni site, instead the Zn occupancy was fixed to the nominal content, due to the very close X-ray scattering power of Ni and Zn ions.

A Labram Dilor Raman spectrometer HD10, equipped with Olympus microscope HS BX40, was employed to perform micro-Raman experiments. The beam of a He–Ne laser at 632.8 nm was focused on a surface of about 2 μm diameter and the scattered light was collected through the same microscope objective, thus conforming a nearly back-scattering geometry. The Raman spectra were recorded by a multi-channel diode array detector. The polarization of the incident light was parallel to the x–y stage, on which the samples were mounted. The laser power was kept low enough (~1 mW) to avoid overheating and degradation of the probed volume and all the measurements were made at room temperature.

3. Results and discussion

In Fig. 1, the diffraction profiles of Mg substituted samples are reported: the main phase is represented by the peaks pertinent to the Y_2BaNiO_5 compound with orthorhombic *Immm* sg C-6 coordination. Small amount of Y_2O_3 and Y_2BaO_4 impurities are observed. A complete and easy substitution of Mg on the Ni site is observed in the investigated compositional range ($0 < x \leq 0.30$).

In Fig. 2, two selected angular ranges of the diffraction patterns of Zn substituted samples are shown: for $x \leq 0.10$ different peaks are observed pertinent to both C-5 and C-6 phases. For $x < 0.15$ the peaks characteristic of the C-5 phase increase their intensity with increasing x, while those of the C-6 phase decrease, suggesting that the *Pnma* polymorph increases its amount until it represents the unique phase for $x \geq 0.15$. The data clearly show that the C-5 polymorph, pertinent to the Y_2BaZnO_5 compound [19], is stable also for low Zn-doping in Y_2BaNiO_5.

Tables 1 and 2 report some results of Rietveld refinement for Mg and Zn substituted samples, respectively. The discrepancy factor (R_{wp}) and the goodness of fit (χ^2) values

Table 1

x	0.05	0.10	0.30
R_{wp}/χ^2	13.79/1.96	13.92/1.77	13.35/1.74
a (Å)	3.7606(1)	3.7593(1)	3.7586(1)
b (Å)	5.7612(1)	5.7627(1)	5.7662(1)
c (Å)	11.3352(1)	11.3357(1)	11.3476(1)
x_{ref}	0.08(2)	0.14(2)	0.29(2)
%C-6 phase	96	97	94
% Impurity	4	3	6

[21] are satisfactory and comparable for all the doped samples. Small amount of impurity phases (Y_2O_3 and Y_2BaO_4), higher for Mg substitution, has been estimated for both series of samples. For Mg doped samples, the lattice parameter values show a very slight change and the cell volume slightly increases with x. The x value, obtained by the site occupancy refinement (x_{ref}), is in good agreement with the nominal concentration especially for high Mg content. For the Zn substituted samples, the lattice parameters of the C-6 phase are quite independent of x, while those of C-5 phase gradually increase. The abundance of C-5 phase (Table 2) increases with x according with previous results [19]. On the basis of the constant values of the C-6 lattice parameters we can argue that very small amount of Zn ions should substitute into Ni site of this polymorph. So, assuming no Zn substitution for $x \leq 0.10$ in C-6 phase and knowing the pertinent phase abundances (Table 2) the amount of the Zn substitution in C-5 phase can be calculated, resulting $Y_2BaNi_{0.861}Zn_{0.139}O_5$ and $Y_2BaNi_{0.873}Zn_{0.127}O_5$ for $x = 0.05$ and 0.10 samples, respectively. These results agree with the solid solution stability limit of about 0.13 [19] for C-5 *Pnma* structure.

For what concerns the Raman scattering, some structural and crystallographic considerations must be taken into account. Both *Immm* and *Pnma* sg are orthorhombic with the D_{2h} point group, but with a different number of formulas in the primitive cell ($Z = 2$ and 4, respectively). Thus, the number of active normal modes is very different for the two

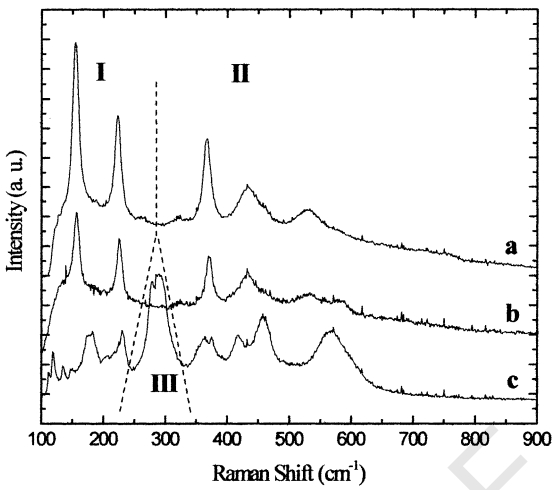

Fig. 3. Raman spectra of (a) Y_2BaNiO_5, (b) $Y_2BaNi_{0.70}Mg_{0.30}O_5$ and (c) $Y_2BaNi_{0.35}Zn_{0.65}O_5$. The three peculiar frequency regions are indicated (see text).

structures. The factor group analysis of the *Immm* structure [23] gives nine allowed Raman modes with $\Gamma = 3A_g + B_{1g} + 2B_{2g} + 3B_{3g}$. In this highly symmetric structure, the Ni, O(2) and Ba ions are located at inversion centres, so they do not contribute to any Raman mode. The structure with the *Pnma* sg has a large primitive cell with 36 ions and 108 normal modes of vibration: among them 52 are Raman active and 35 are IR active [24].

Fig. 3 shows the Raman spectra for the pure Y_2BaNiO_5 (a), $Y_2BaNi_{0.7}Mg_{0.3}O_5$ (b) and $Y_2BaNi_{0.35}Zn_{0.65}O_5$ (c), respectively. The spectrum of Y_2BaNiO_5 is in good agreement with previous literature [23]. It is widely accepted [23,25] that the spectrum can be divided into two regions. The lower (I), below 250 cm^{-1} shows peaks due to vibrations involving the rare earth ion, while the higher region (II), above 350 cm^{-1}, shows the scattering due to vibrations involving the O(1) sublattice which forms the basal planes of the Ni–O octahedra. In Fig. 3 one can clearly observe, for Mg and pure samples, five Raman modes

Table 2

x	0.05	0.10	0.15	0.30	0.65
R_{wp}/χ^2	13.05/1.69	13.23/1.66	13.02/1.51	12.71/1.39	13.64/1.74
C-6 phase					
a (Å)	3.7587(1)	3.7573(1)	3.7569(13)		
b (Å)	5.7632(1)	5.7621(1)	5.7656(28)		
c (Å)	11.3408(1)	11.3405(1)	11.3305(59)		
Percentage	64	21	0.5		
C-5 phase					
a (Å)	12.2826(1)	12.2822(1)	12.2872(1)	12.2943(1)	12.3158(1)
b (Å)	5.6902(1)	5.6896(1)	5.6918(1)	5.6943(1)	5.7017(1)
c (Å)	7.0264(1)	7.0270(1)	7.0307(1)	7.0373(1)	7.0542(1)
Percentage	35	78	95.5	99	99
% Impurity	1	1	4	1	1

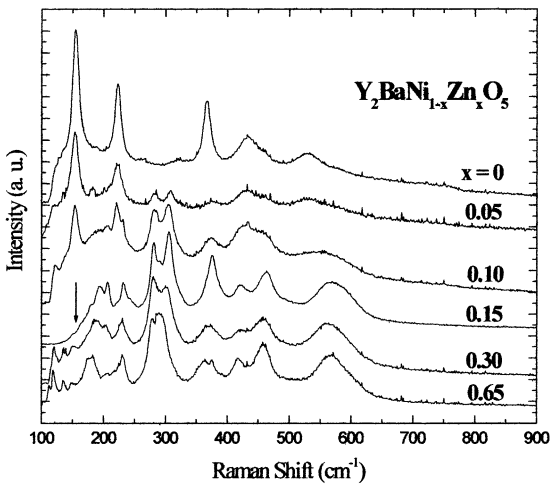

Fig. 4. Raman spectra of Zn doped samples. The arrow on the spectrum of $x = 0.15$ sample indicates the different cut-off due to the optical set-up of the notch filter.

peaked, respectively, at 155, 223, 367, 432 and 532 cm^{-1}, the last two features being weaker and broadened. There is an additional mode at lower energy around 110 cm^{-1}, more clear in Zn doped samples, whose shape is, however, strongly affected by the cut-off of the notch filter. We recall briefly that: (i) the peaks at 155 and 223 cm^{-1} correspond to the B_{3g} and A_g modes due to Y motion; (ii) the peaks above 350 cm^{-1} are due to the B_{3g} and A_g O(1) modes [24,25]. In addition, Raman spectrum of the pure sample reveals a weak feature around 750 cm^{-1}, which corresponds to the infrared Ni–O(2) stretching mode, Raman forbidden but activated by the disorder [23].

According to structural data, Mg substitution does not cause heavy changes in the vibrational spectrum, as it can be deduced from Raman spectra of $x = 0.05$, 0.10, and 0.30 samples. The peak position and the relative intensities of the different modes remain almost unchanged (see Fig. 3(b) for $x = 0.30$ sample), being the B_{3g} mode, due to Y motion, the most intense. Nevertheless we notice that in the region II, i.e. the region of oxygen vibrations, the higher energy band, centred at 532 cm^{-1} as in the pure compound (Fig. 3(a)) is accompanied by a shoulder peaked at 583 cm^{-1} in the Mg sample. We can attribute this peak to O(1) vibrations inside the Mg–O(1) plane, where the different mass and charge of the cation may induce the observed small differences with respect to Ni–O(1) planes.

Fig. 3(c) clearly shows that the substitution of Ni by Zn causes significant changes in the Raman spectrum. At first, the distribution of the intensities is completely different. The low energy part of the spectrum changes markedly and in general a greater number of Raman lines is observed according to the structural data and the factor group analysis mentioned earlier. In particular, the main difference can be considered the appearance of Raman peaks in the range 260–340 cm^{-1} (region III in Fig. 3). This is considered a clear marker of the *Pnma* phase and we will discuss this region with more details later.

In order to clear up the role of Zn in the vibrational spectrum, when it substitutes progressively Ni ions, we measured the $Y_2BaNi_{1-x}Zn_xO_5$ compounds. The results are shown in Fig. 4. Considering the modes involving the rare earth we observe that the mode at 155 cm^{-1} in the pure sample decreases strongly its intensity with increasing Zn content and undergoes to a weak softening. In particular, the strong increase of C-5 phase causes a quick decrease in its intensity, as clearly shown passing from $x = 0.05$ to 0.10. A new broad structure appears at 175 cm^{-1} starting from $x = 0.10$. The peak at 233 cm^{-1} decreases linearly its intensity and the frequency slightly hardens, passing from 223.8 cm^{-1} in $x = 0.05$ to 231.4 cm^{-1} in 0.65.

In region II, we observe an increase in the vibrations energy with increasing Zn content. In $x = 0.05$ sample the energy of the A_g mode (536 cm^{-1}) is slightly increased with respect to that in pure compound, but it progressively increases up to 570 cm^{-1} in the heavy substituted sample. This behaviour is in agreement with the fact that in the C-5 phase the Ni–O distances are markedly different from those of C-6 phase. Indeed, in *Immm* phase we have Ni–O(1) = 2.18 Å and Ni–O(2) = 1.88 Å, while in *Pnma* phase the Ni–O distances are closer and range between 1.98 and 2.07 Å as deduced by atomic positions refinement of diffraction data. For this reason, one can expect the stretching modes of oxygen having higher energy in the *Pnma* phase, due to the behaviour of the force constants on the interatomic distances [23]. The upper energy limit for this type of vibrations corresponds to the energy of the infrared stretching mode of about 750 cm^{-1}. Furthermore we observe the intensity decrease of the symmetric A_g mode and the splitting of the anti-symmetric B_{3g} mode in two components centred at 415 and 458 cm^{-1} in $x = 0.65$. This is probably due to the different M–O bond distances in the C-5 pyramidal polyhedra.

Finally, let us discuss the characteristic region III of the *Pnma* phase between 260 and 340 cm^{-1}. It was previously proposed that the peaks in this interval are due to the motion of M ion [23]; this lattice site loses the inversion symmetry leading to active Raman vibrations. Indeed even in $x = 0.05$ sample the appearance of two components is evident though the intensity of the spectrum is very weak. Increasing the Zn content, the relative intensity increases much more with respect to the other peaks of the spectrum and the two components, clearly detectable in $x = 0.10$, become the most intense modes of the observed Raman scattering interval. A detailed analysis of the spectra was performed by fitting the data to a superposition of Lorentzian curves. The best-fit values for the energy and the integrated intensities are shown in Fig. 5. Our goal is to correlate the observed features with the content of Zn and to establish a relationship between the sum of the integrated intensities of the Raman modes in this region and the amount of C-5 phase deduced from XRD data.

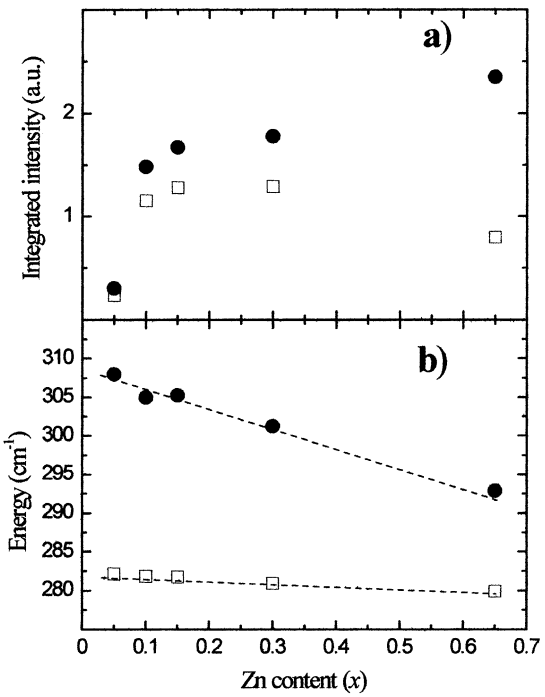

Fig. 5. Best-fit values for (a) integrated intensities and (b) energies of the C-5 Raman modes of region III as a function of Zn content. The dashed lines are eye guides.

At this purpose we assume the sum of the two components of the Raman spectrum for $x = 0.65$ sample equivalent to the 100% C-5 phase (known from XRD data) and rescale the Raman results to this value. Fig. 6 shows the resulting values estimated from XRD and Raman experiments as a function of x. There is a good agreement between the two sets of data, suggesting that the sum of the integrated intensities of the considered modes can effectively constitute a good tool to estimate the abundance of C-5 phase.

Moreover, we try to gain new insight on the nature of these modes whose values of energy and integrated intensity are shown in Fig. 5. The frequency of the high energy peak shifts towards lower value passing from 307.5 cm^{-1} in $x = 0.05$ to 292.5 cm^{-1} in the $x = 0.65$ sample, while the frequency of the lower energy peak remains unchanged. The intensity of the two components shows different behaviour: the high energy component increases while the lower energy one decreases with increasing x. Considering that such modes are due to vibrations of metal ions in the M–O bond we can suggest that the cation is directly involved in the high energy mode. The heavier Zn causes the observed softening of the energy, when it progressively substitutes Ni. It can be hypothesized that the low energy mode involves preferentially Ni ions while the high energy mode is mainly due to the vibrations of Zn. This may justify the observed behaviour for the integrated intensities.

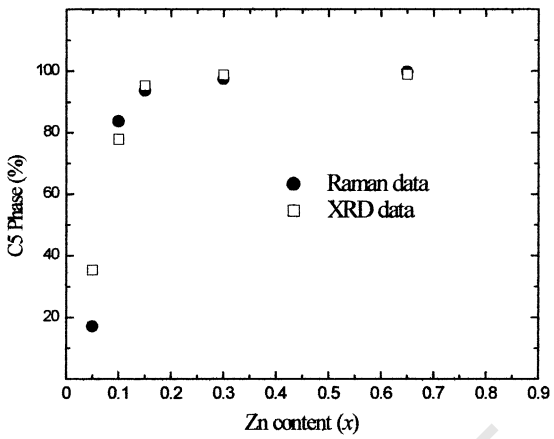

Fig. 6. C-5 phase abundance as a function of Zn content as estimated from XRD and Raman data.

4. Conclusions

These results show that the analysis of combined XRD and Raman spectroscopy data allows to put into evidence the different trends occurring in the Y_2BaNiO_5 compound when Mg^{2+} and Zn^{2+} cations are substituted into the Ni site. In fact, this work examines both the case of the *Immm* structure preservation (Mg-doping) and the case of evolution towards the new *Pnma* polymorph (Zn-doping).

For Mg-doping, no structural change occurs and only a gradual, very slight lattice expansion is observed, and the Raman spectrum remains practically unchanged.

For Zn-doping, the structural changes and the transition towards a C-5 coordination phase lead to marked variations with respect to the pure compound, clearly observable with both techniques. In particular, it is observed that samples with lower Zn-doping level ($0 < x \leq 0.10$) show the coexistence of the two polymorphs (C-5 and C-6 coordination), with Zn ion occupying only the Ni site of C-5 phase. For higher Zn content ($0.15 \leq x \leq 0.65$), only the C-5 phase is present. This fact clearly reflects on Raman spectra, where the phase transformation implies the disappearance of the inversion symmetry for the metal ion sites, with peculiar Raman modes in the intermediate frequency region (260–340 cm^{-1}). The integrated intensities of the modes are used to estimate the phase abundance and the results are satisfactorily compared with those deduced from XRD. Finally, the behaviour of energy and intensity of these Raman modes vs. the Zn content allows us to discuss a possible interpretation of the nature of these modes.

Acknowledgments

This work has been partially supported by ‘Consorzio per i Sistemi a Grande Interfase’ (CSGI) and ‘Istituto per l’Energetica e le Interfasi’ (IENI) of CNR.

References

[1] J. Darriet, L.P. Regnault, Solid State Commun. 86 (1993) 409.
[2] T. Yokoo, T. SuKaguchi, K. Kakurai, J. Akimitsu, J. Phys. Soc. Jpn 64 (1996) 3651.
[3] M. Merli, D. Capsoni, M. Bini, V. Massarotti, Solid State Commun. 121 (2002) 193.
[4] D.J. Buttrey, J.D. Sullivan, A.L. Rheingold, J. Solid State Chem. 88 (1990) 291.
[5] N. Ogita, Y. Tsunezumi, T. Yokoo, J. Akimitsu, M. Udagawa, J. Phys. Soc. Jpn 66 (1997) 873.
[6] P.E. Sulewski, S.W. Cheong, Phys. Rev. B 51 (1995) 3021.
[7] A. Salinas-Sanchez, R. Saez-Puche, F. Fernandez, A. de Andres, A.E. Lavat, E.J. Baran, J. Solid State Chem. 99 (1992) 63.
[8] M. Taibi, J. Aride, J. Darriet, A. Moqine, A. Boukhari, J. Solid State Chem. 86 (1990) 233.
[9] M. Taibi, J. Aride, E. Antic-Fidancev, M. Lemaitre-Blaise, P. Porcher, P. Caro, J. Solid State Chem. 74 (1988) 329.
[10] P.E. Sulewski, S.W. Cheong, Phys. Rev. B 50 (1994) 551.
[11] C. Michel, B. Raveau, J. Solid State Chem. 49 (1983) 150.
[12] E. Garcia-Matres, J.L. Martinez, J. Rodriguez-Carvajal, J.A. Alonso, A. Salinas-Sanchez, R. Saez-Puche, J. Solid State Chem. 103 (1993) 322.
[13] V. Massarotti, D. Capsoni, M. Bini, A. Altomare, A.G.G. Moliterni, Z. Kristallogr. 214 (1999) 205.
[14] F. Tedoldi, A. Rigamonti, C. Brugna, M. Corti, A. Lascialfari, D. Capsoni, V. Massarotti, J. Appl. Phys. 83 (1998) 6605.
[15] F. Tedoldi, A. Rigamonti, R. Santachiara, M. Horvatic, L. Linati, M. Bini, D. Capsoni, V. Massarotti, Appl. Magn. Res. 19 (2000) 381.
[16] B. Batlogg, S.W. Cheong, L.W. Rupp, Physica B 194 (1994) 173.
[17] J.F. Ditusa, S.W. Cheong, C. Broholm, G. Aeppli, C.W. Rupp, J.R, B. Batlogg, Physica B 104–106 (1994) 181.
[18] F.J. Mompean, M. Garcia Hernandez, J.L. Martinez, E. Garcia Matres, C. Prieto, A. de Andres, R. Saez-Puche, R.S. Eccleston, H. Schober, Physica B 234–236 (1997) 572.
[19] R. Saez-Puche, J.M. Coronado, C.L. Otero-Diaz, J.M. Martin Llorente, J. Solid State Chem. 93 (1991) 461.
[20] H.M. Rietveld, J. Appl. Crystallogr. 2 (1969) 65.
[21] J. Rodriguez-Carvajal, Physica B 192 (1993) 55.
[22] V. Massarotti, D. Capsoni, M. Bini, Z. Naturforsch 51a (1996) 267.
[23] A. de Andres, J.L. Martinez, R. Saez-Puche, A. Salinas-Sanchez, Solid State Commun. 82 (1992) 931.
[24] A. de Andres, S. Taboada, J.L. Martinez, A. Salinas, J. Hernandez, R. Saez-Puche, Phys. Rev. B 47 (1993) 14898.
[25] M.V. Abrashev, M.N. Iliev, Phys. Rev. B 45 (1992) 8046.